



Facile Synthesis and Characterization of Pure and Bi-doped ZnS Nanoparticles for Photocatalytic Application

T. Shobana¹, T. Venkatesan¹, R. Sakthi Sudar Saravanan¹, D. Kathirvel^{2*} and K. Valliyammal¹

¹Department of Physics, Chikkanna Government Arts College, Tiruppur, TN, India

²Department of Physics, Government Arts College, Coimbatore, TN, India

Received: 26.06.2024 Accepted: 05.09.2024 Published: 30.09.2024

*kathirvelde@gmail.com

ABSTRACT

In the present research, a simple solvothermal microwave irradiation (SMI) method has been adopted for the preparation and synthesis of pure and Bi doped ZnS nanoparticles using zinc acetate, bismuth acetate, thiourea and ethylene glycol were utilized as precursors. As-synthesized pure and Bi doped ZnS nanoparticles were characterized by X-ray diffraction (XRD), energy dispersive X-ray spectroscopy (EDAX), ultraviolet-visible (UV-vis) spectroscopy and Field emission scanning electron microscopy (FESEM). From the XRD and EDAX studies, crystallite size, lattice parameter and analysis of the elemental compositions are calculated and analyzed respectively. The UV-vis spectra revealed that the optical band gap energy of pure and Bi doped ZnS nanoparticles was calculated. The FESEM shows that the average particle size spherical and agglomerated of as-synthesized pure and Bi doped ZnS nanoparticles sizes were decreased. In addition, the photocatalytic activity of pure and Bi doped ZnS nanoparticles was studied with methylene blue dye in an aqueous solution under UV light irradiation; the 5.0 mol % of Bi doped ZnS nanoparticles dye degradation efficiency of the sample was calculated as 75% in 120 minutes.

Keywords: ZnS nanoparticles; Microwave irradiation method; Photocatalytic degradation; Methylene blue dye.

1. INTRODUCTION

In the modern world, excessive usage and mishandling of chemicals in many developed industries, such as textile dyeing units and paramedical sectors, release chemical effluents that act as chemical pollutants in our environment. It causes air pollution, water pollution, soil pollution, etc. To eliminate the presented chemical pollutants/contaminants from the environment, water purification from contaminated water is a most urgent need to address the present scenario. Using semiconductor nanoparticles is an instant remedy for the above-addressed issue; particularly, zinc sulfide (ZnS) nanoparticles aid in preventing chemical pollutants from entering water systems. ZnS - face-centered cubic structure - is an essential, direct, and significantly large band gap energy of 3.63–3.92 eV semiconductor material in the II-VI group, which exhibits distinct features, including a large ionization transition and phase stability under typical atmospheric circumstances (Mani *et al.* 2018; Shobana *et al.* 2020). Primarily, they possess optical characteristics such as long retention time, strong light absorption, long electron-hole recombination time, high negative reduction-oxidation potential of excited electrons, and the ability to produce significant electron-hole pairs (Reza Gholipour *et al.* 2015; Yang *et al.* 2015). Therefore, ZnS nanoparticles perform effectively as photocatalysts and are helpful for filtering chemicals

before releasing them into the environment. They also show good antibacterial activity. In the preparation of ZnS nanoparticles, numerous methods have been employed by many research scholars (Calandra *et al.* 1999; Charinpanitkul *et al.* 2005; Jadraque *et al.* 2013; Yu *et al.* 2013; Shanmugam *et al.* 2014; Tounsi *et al.* 2018; Sabaghi *et al.* 2018; Palve, 2019; Altiokka *et al.* 2019; Goktas *et al.* 2019; Elsi *et al.* 2021; Rose *et al.* 2022; Bui *et al.* 2023). Among these, the solvothermal microwave irradiation (SMI) method (Shahid *et al.* 2012) is highly controllable, productive, and does not require the operation of calcination or grinding. Various elements (Ag, Cd, Fe, In, Mg, Mn, and Ni) serve as dopants of ZnS nanoparticles, which enhance the ZnS performance and are reported by various researchers (Zhang *et al.* 2011; Khorsand Zak *et al.* 2012; Ramasamy *et al.* 2012; Al-Rasoul *et al.* 2013; Sousa *et al.* 2018; Othman *et al.* 2020; Jindal *et al.* 2021; Rana *et al.* 2021; Bui *et al.* 2023; Dixit *et al.* 2015; Dhupar *et al.* 2021; Ashokkumar *et al.* 2018; Ashokkumar *et al.* 2018; Hussein M. Hussein, 2023; Khan *et al.* 2024; Kalantari *et al.* 2024) Bi based photocatalysts some researchers have summarized and reported (Bi₂S₃ and other bi-based photocatalyst), including their uses for the removal of organic pollutants, hydrogen production, oxygen production, etc. (Song *et al.* 2023). The present research work focused on synthesizing pure and Bi doped ZnS nanoparticles, examined their structural and optical

properties, and then utilized them to investigate the effects of photocatalytic activities.

2. EXPERIMENTAL METHODS

2.1 Materials

For synthesizing the pure and Bi doped ZnS nanoparticles, all the chemicals - zinc acetate ($\text{Zn}(\text{CH}_3\text{COO})_2 \cdot 2\text{H}_2\text{O}$ - as the source of Zn), thiourea ($\text{CH}_4\text{N}_2\text{S}$ - as the source of S), bismuth acetate ($\text{Bi}(\text{CH}_3\text{COO})_3$ - as the source of Bi) and ethylene glycol ($\text{C}_2\text{H}_6\text{O}_2$) - are of AR grade purchased from Sigma Aldrich in India.

2.2 Synthesis and Preparation of ZnS Nanoparticles

To synthesize pure ZnS nanoparticles, zinc acetate and thiourea were initially dissolved separately in 50 ml of ethylene glycol under stirring for an hour at room temperature. Both dissolved 50 ml solutions were gradually mixed and made into a 100 ml precursor solution under the stirring condition for homogeneity. The prepared 100 ml precursor was transferred to a bowl and placed in the domestic microwave oven to form a colloidal precipitate. The microwave oven has been maintained at the operating frequency of 2.45 GHz and has a 50% power cycle controlled to prevent solvent evaporation. The formed colloidal precipitate was allowed to cool and settle naturally at room temperature; then, it was thoroughly cleaned with double-distilled water, and acetone was utilized to remove any possible unreacted precursors and residual impurities. The final product was stored for six hours in a hot air oven at 80 °C after being centrifuged for ten minutes at 10,000 rpm. A similar process was adopted for the synthesis of 2.5 mol % and 5.0 mol % of bismuth-doped ZnS nanoparticles, and finally, the synthesized samples were collected and coded as Pure ZnS, 2.5 mol % Bi-doped ZnS and 5.0 mol % Bi-doped ZnS.

3. RESULTS AND DISCUSSION

3.1 XRD - Structural Analysis

XRD pattern of synthesized ZnS nanoparticles is the cubic structure depicted in Fig. 1. The Bragg peaks ($2\theta = 28.6, 47.5$ and 56.4) in the patterns obtained from XRD are (111), (220), and (311) planes which exhibited good agreement with the standard pattern (JCPDS No. 65-0309) (Dixit *et al.* 2015). When the (2.5 mol % and 5.0 mol %) dopant concentration increases, the peak intensity in Fig. 1 inferred that the broadening of the diffraction peaks indicates the extremely tiny size of the grains. For the most intense peak (111) plane, the size of the pure and Bi doped ZnS nanoparticles crystallites was determined using Debye Scherrer's equation (Shobana *et al.* 2024).

The lattice parameters ($a=b=c$) for face centered cubic structured ZnS nanoparticles have been calculated using the following equation (Ali *et al.* 2022).

$$\frac{1}{d_{hkl}^2} = \frac{h^2 + k^2 + l^2}{a^2} \quad (1)$$

where, d_{hkl} is the interplanar spacing distance (Å) corresponding to Miller indices (hkl) and a is the lattice parameter (Å). The calculated lattice parameter, unit cell volume and average crystallite size (D) of pure and Bi doped ZnS nanoparticles are presented in Table 1.

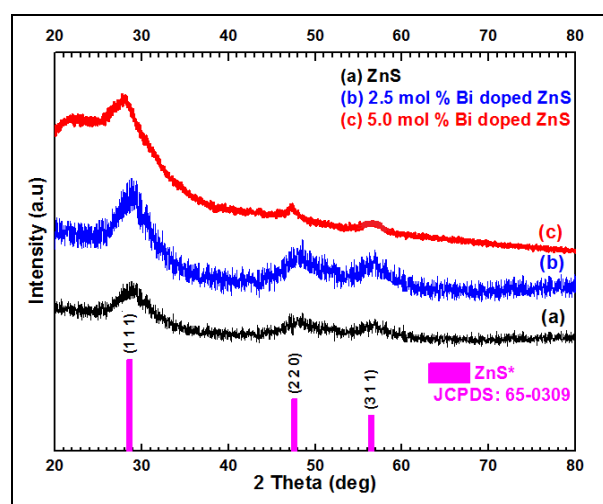


Fig. 1: XRD pattern of ZnS Nanoparticles (a) Pure ZnS (b) 2.5 mol % Bi doped ZnS (c) 5.0 mol % Bi doped ZnS Nanoparticles

Table 1. XRD structural parameters of Pure ZnS, 2.5 mol % and 5.0 mol % Bi doped ZnS Nanoparticles

Sample	Lattice parameter $a=b=c$ (Å)	Unit cell volume (Å) ³	Average crystallite size D (nm)
Pure ZnS	5.392	156.76	3.34
2.5 mol % Bi doped ZnS	5.386	156.24	3.98
5.0 mol % Bi doped ZnS	5.381	155.80	5.04

3.2 EDAX Spectra Analysis

EDAX spectra of pure and Bi doped ZnS nanoparticles were obtained and the chemical compositions in the atomic % of Zn, Bi and S also mentioned in Fig. 2. It shows the sample was in good agreement and purity in the elemental compositions as the researcher considered in this work. In addition, the presence of dopant was confirmed by the EDAX spectra, which also demonstrated the processed samples purity.

3.3 FESEM Analysis

FESEM analysis was utilized for the morphological analysis of pure and Bi doped ZnS nanoparticles. FESEM images show agglomerated,

spherically-shaped pure and Bi doped ZnS nanoparticles as shown in Fig. 3.

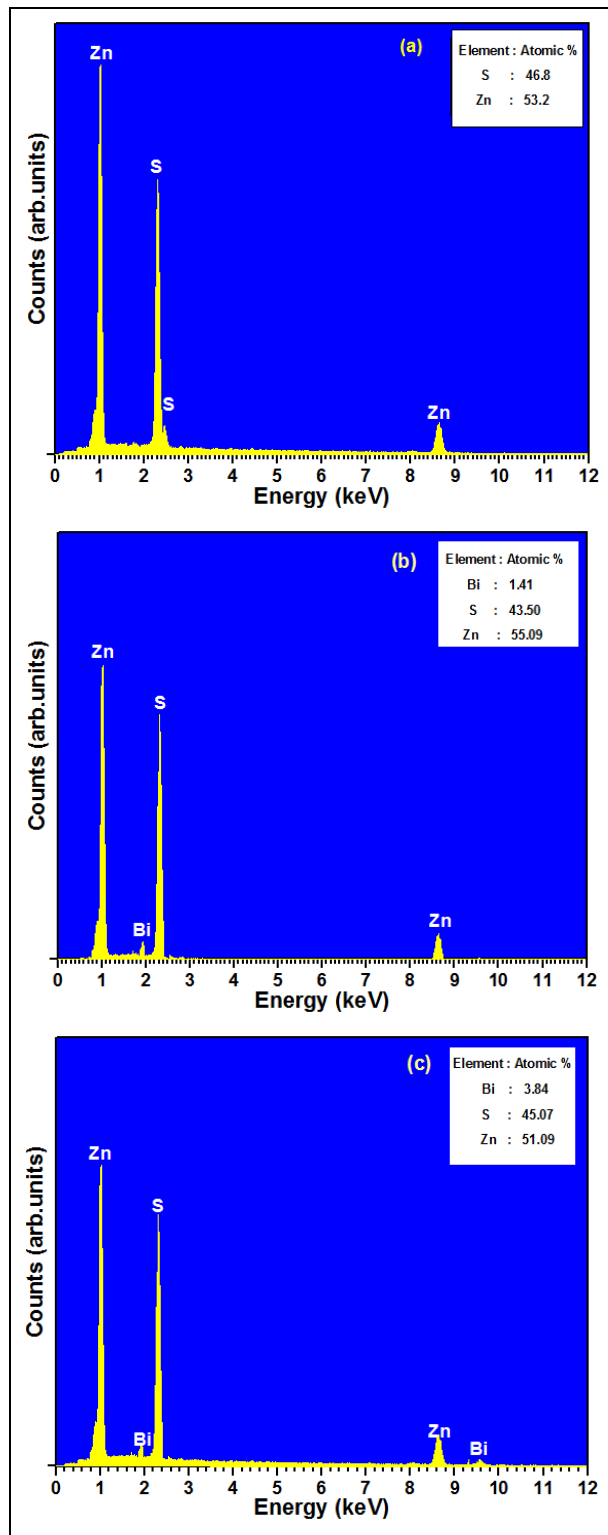


Fig. 2: EDAX spectra of ZnS Nanoparticles (a) Pure ZnS (b) 2.5 mol % Bi doped ZnS (c) 5.0 mol % Bi doped ZnS Nanoparticles

From the Fig. 3 inferred that the existence of spherical agglomerates made up of individual

nanoparticles with consistent shapes and sizes were measured (Ali *et al.* 2022) with the ImageJ tool. As-synthesized pure and Bi doped ZnS nanoparticle sizes were calculated in the range of 62 nm to 78 nm.

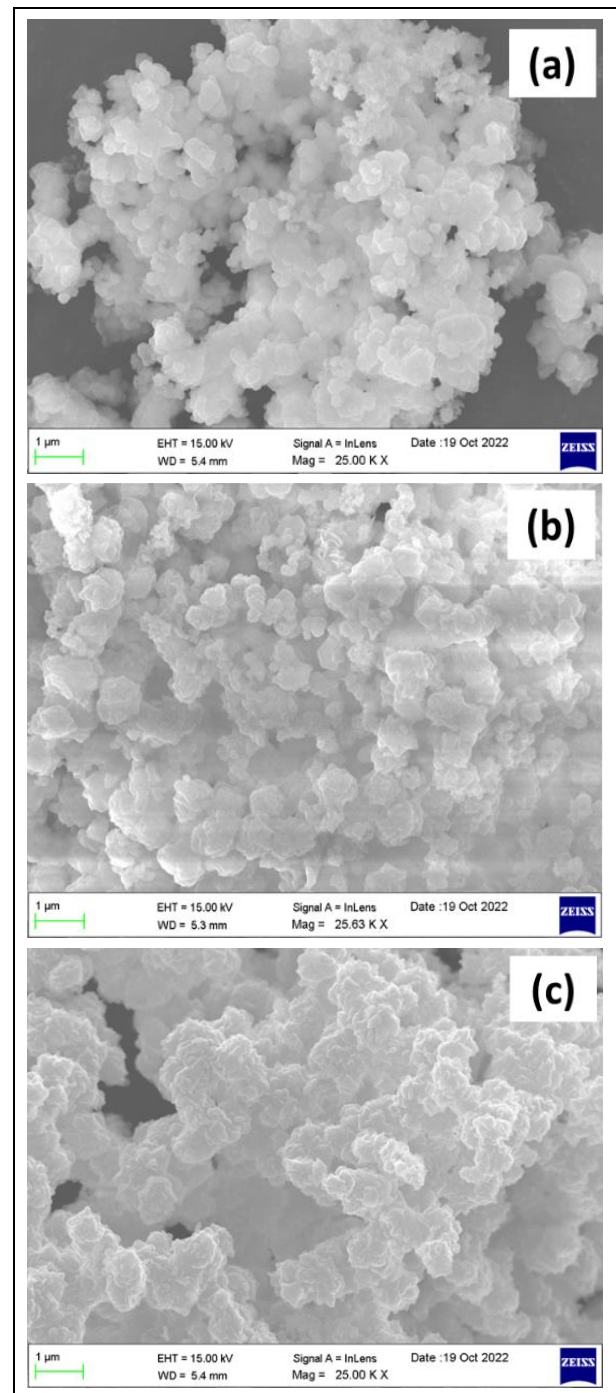


Fig. 3: FESEM images of nanoparticles (a) Pure ZnS (b) 2.5 mol % Bi doped ZnS (c) 5.0 mol % Bi doped ZnS Nanoparticles

3.4 UV-visible analysis

UV-vis spectra of pure and Bi doped ZnS nanoparticles as given in Fig. 4, which also shows the obtained band gap energy value (eV) using Tauc's plot,

which plotted between $(\alpha h\nu)^2$ and energy (Bhat *et al.* 2024). The obtained direct band gap energy (eV) of synthesized pure ZnS, 2.5 mol % Bi doped ZnS and 5.0 mol % Bi doped ZnS nanoparticles are found 3.56 eV, 3.52 eV and 3.47 eV (Wang *et al.* 2020).

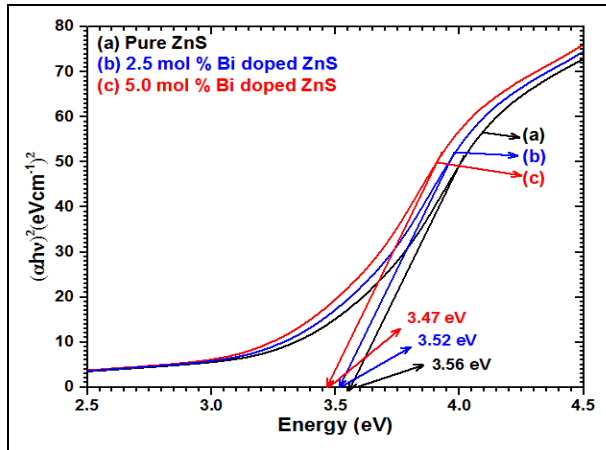


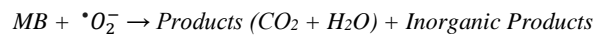
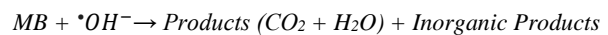
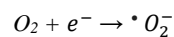
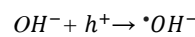
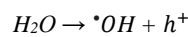
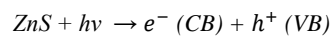
Fig. 4: UV-vis analysis of (a) Pure ZnS (b) 2.5 mol % Bi doped ZnS (c) 5.0 mol % Bi doped ZnS Nanoparticles

4. PHOTOCATALYTIC ACTIVITY

4.1 Photocatalytic Mechanism

A UV light was exposed to as-synthesized ZnS nanoparticles; it produces free electrons in the valence

band that is subsequently transferred to the conduction band, leaving holes in the valence band. While the holes in the h^+ valence band can promptly move to the e^- valence band, the electrons in the h^+ conduction band can migrate to that of the e^- in the valence band. It is possible to separate photogenerated carriers (electrons and holes) efficiently and extend their effective period throughout the electron and hole migration process. In order to accomplish the goal of degradation, the photogenerated electrons can also interact with O_2 to produce $^*O_2^-$ and then subsequently react with contaminants (Lee *et al.* 2017). Finally, the products obtained from the photogenerated holes ($^*OH^-$) and electrons ($^*O_2^-$) directly break down and oxidize methylene blue dye, resulting in its degradation into CO_2 and H_2O .



A complete photocatalytic mechanism as an equation is depicted in Fig. 5 (Shobana *et al.* 2024).

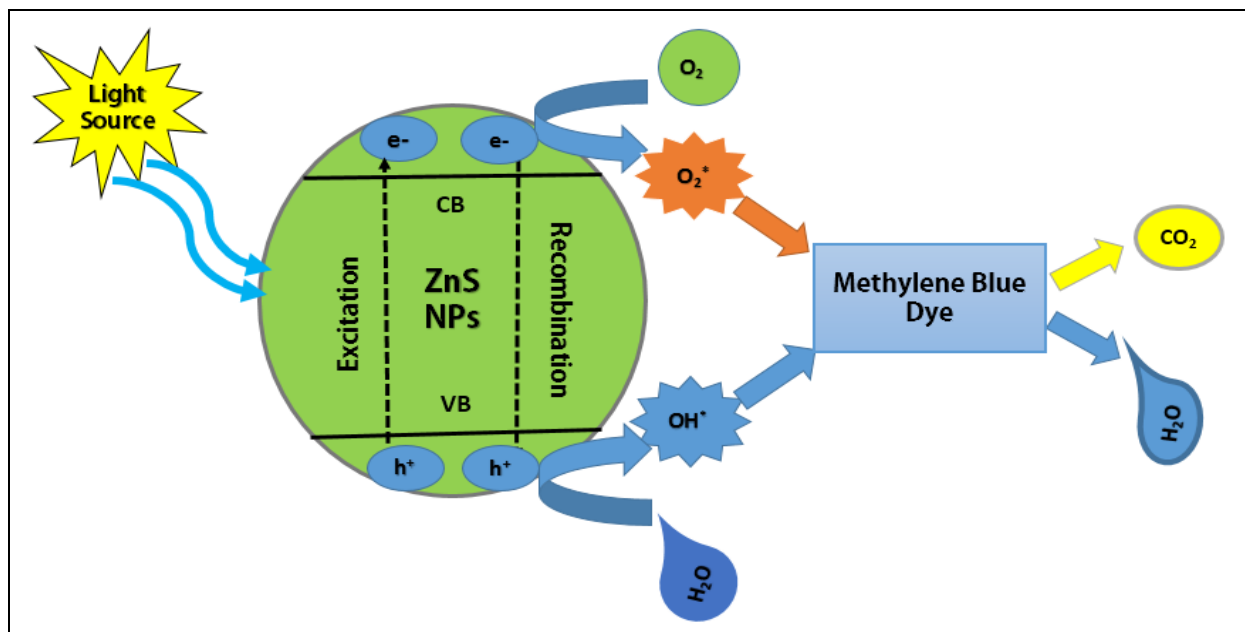


Fig. 5: Photocatalytic mechanism of ZnS nanoparticles with methylene blue dye

4.2 Photocatalytic Results

The methylene blue dye was used to examine the photocatalytic activity of synthesized pure and Bi doped ZnS nanoparticles. The photocatalytic study of pure and Bi doped ZnS nanoparticles has been involved

with the MB dye with fixed concentrations (10 ppm) and catalytic dosage (10 mg/L). Samples were taken at regular intervals of every 30 minutes to ensure that the catalyst suspension remained constant during the reaction for the degradation tests under exposure to UV light radiation. The UV absorbance of each samples were

graphically represented in figure 6 and then evaluated and calculated the percentage of methylene blue dye degradation efficiency and the photocatalytic kinetic rate constants were calculated and found to be 1.2×10^{-3} , 1.3×10^{-3} and $1.5 \times 10^{-3} \text{ min}^{-1}$ for pure ZnS, (2.5 and 5.0) mol % of ZnS nanoparticles, respectively; using a linear relation by the pseudo-first-order kinetic model and the relations as follows, (Mani *et al.* 2018; Riazian *et al.* 2020; Shobana et al. 2024).

$$\eta = \frac{A_0 - A_t}{A_0} \times 100\% \quad (2)$$

$$\ln\left(\frac{A_0}{A_t}\right) = kt \quad (3)$$

where A_0 is the initial dye degradation concentration and A_t is the final dye degraded concentration at time ($t = 0, 30, 60, 90$ and 120 minutes) (Wang *et al.* 2020).

5. CONCLUSION

Pure ZnS and Bi doped ZnS nanoparticles were successfully synthesized using a simple microwave irradiation technique. The prepared nanoparticles were characterized and calculated; the average crystallite size was found to be 4.12 nm with a face-centered cubic crystallite structure nature by XRD; the obtained EDAX spectra show that the chemical composition of Zn, Bi and S elements, the average particle size was found to range of 62 nm to 78 nm calculated from FESEM with a spherical shape, UV-vis absorption spectra were analyzed using Tauc plots and the optical energy band gap was found for pure and Bi doped ZnS nanoparticles and their ranges from 3.47 to 3.56 eV . As-synthesized ZnS nanoparticles are effectively employed for the removal of the chemical pollutant – methylene blue dye – under UV light irradiation by the photocatalytic process. The (5.0 mol %) Bi doped ZnS efficiency of dye degradation of methylene blue was achieved 75 % in 120 minutes. Hence, the present study suggests that pure ZnS and Bi-doped ZnS nanoparticles act as photocatalysts, and they are promising for the breakdown of harmful organic pollutants in the field of water treatment.

ACKNOWLEDGMENTS

The authors thank characterization techniques done at Coimbatore Institute of Technology (CIT), Coimbatore and Avinashilingam Institute for Home and Higher Education for Women, Coimbatore.

FUNDING

This research received no specific grant from any funding agency in the public, commercial, or not-for-profit sectors.

CONFLICTS OF INTEREST

The authors declare that there is no conflict of interest.

COPYRIGHT

This article is an open-access article distributed under the terms and conditions of the Creative Commons Attribution (CC BY) license (<http://creativecommons.org/licenses/by/4.0/>).

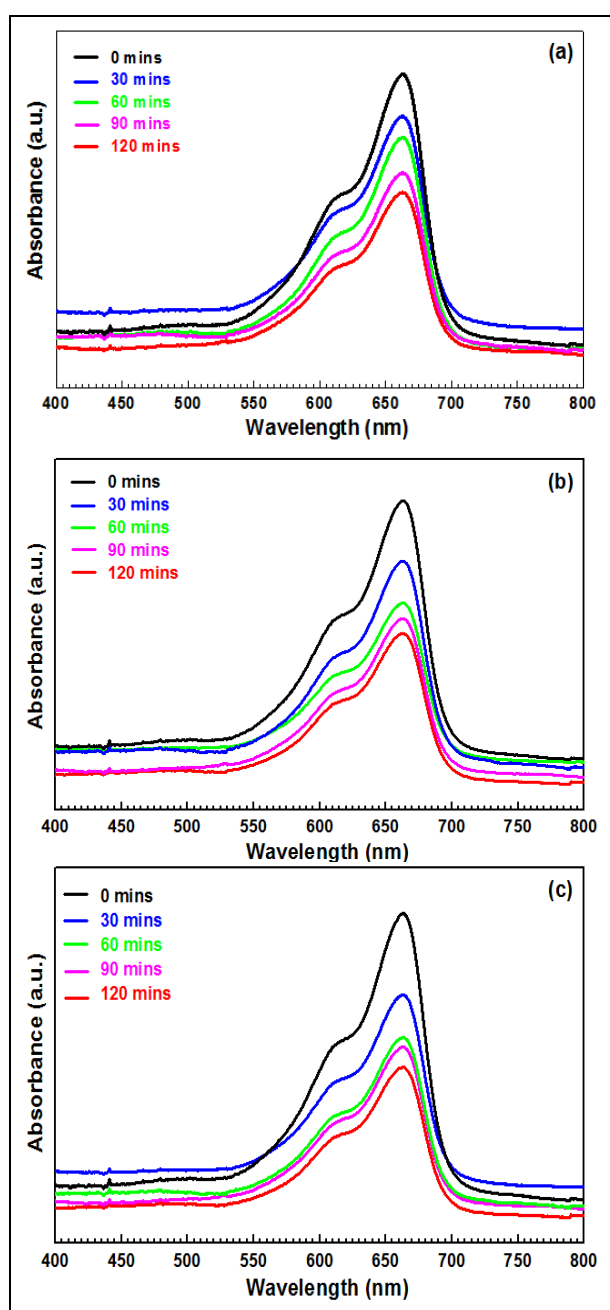


Fig. 6: Photocatalytic activity for methylene blue dye with catalysts (a) Pure ZnS (b) 2.5 mol % Bi doped ZnS (c) 5.0 mol % Bi doped ZnS Nanoparticles

Percentage of dye degradation efficiency



REFERENCES

- Al- Rasoul, K. T., Abbas, N. K., Shanan, Z. J., Structural and Optical Characterization of Cu and Ni Doped ZnS Nanoparticles, *Int. J. Electrochem. Sci.* 8(4), 5594–5604 (2013).
[https://doi.org/10.1016/S1452-3981\(23\)14706-7](https://doi.org/10.1016/S1452-3981(23)14706-7)
- Ali, A. H., Hashem, H. A., Elfalaky, A., Preparation, Properties, and Characterization of ZnS Nanoparticles, *Engineering Proceedings*, 74 (2022).
<https://doi.org/10.3390/ASEC2022-13829>
- Altokka, B., Effects of Inhibitor on ZnS Thin Films Fabricated by Electrodeposition, *J. Electron. Mater.* 48(4), 2398–2403 (2019).
<https://doi.org/10.1007/s11664-019-06950-z>
- Ashokkumar, M., Boopathyraja, A., Structural and optical properties of Mg doped ZnS quantum dots and biological applications, *Superlattices Microstruct.* 113, 236–243 (2018).
<https://doi.org/10.1016/j.spmi.2017.11.005>
- Bhat, B. A., Jadon, N., Dubey, L., Mir, S. A., Facile Synthesis of a Crystalline Zinc Sulfide/Chitosan Biopolymer Nanocomposite: Characterization and Application for Photocatalytic Degradation of Textile Dyes and Anticancer Activity, *ACS Omega* 9(23), 24425–24437 (2024).
<https://doi.org/10.1021/acsomega.4c00247>
- Bui, H. Van, Thai, D. Van, Nguyen, T. D., Lam, V. N., Tran, H. T., Nguyen, V. M., Nui, N. D., Hung, N. M., Mn-doped ZnS nanoparticle photoanodes: Synthesis, structural, optical, and photoelectrochemical characteristics, *Mater. Chem. Phys.* 307, 128081 (2023).
<https://doi.org/10.1016/j.matchemphys.2023.128081>
- Calandra, P., Goffredi, M., Liveri, V. T., Study of the growth of ZnS nanoparticles in water/AOT/n-heptane microemulsions by UV-absorption spectroscopy, *Colloids Surfaces A Physicochem. Eng. Asp.* 160(1), 9–13 (1999).
[https://doi.org/10.1016/S0927-7757\(99\)00256-3](https://doi.org/10.1016/S0927-7757(99)00256-3)
- Charinpanitkul, T., Chanagul, A., Dutta, J., Rungsardthong, U., Tanthapanichakoon, W., Effects of cosurfactant on ZnS nanoparticle synthesis in microemulsion, *Sci. Technol. Adv. Mater.* 6(3–4), 266–271 (2005).
<https://doi.org/10.1016/j.stam.2005.02.005>
- Dhupar, A., Kumar, S., Tuli, H. S., Sharma, A. K., Sharma, V., Sharma, J. K., In-doped ZnS nanoparticles: structural, morphological, optical and antibacterial properties, *Appl. Phys. A* 127(4), 263 (2021).
<https://doi.org/10.1007/s00339-021-04425-9>
- Dixit, N., Vaghasia, J. V., Soni, S. S., Sarkar, M., Chavda, M., Agrawal, N., Soni, H. P., Photocatalytic activity of Fe doped ZnS nanoparticles and carrier mediated ferromagnetism, *J. Environ. Chem. Eng.* 3(3), 1691–1701 (2015).
<https://doi.org/10.1016/j.jece.2015.06.010>
- Elsi, S., Pushpanathan, K., Room temperature ferromagnetism in ZnS and ZnO nanoparticles, *Inorg. Nano-Metal Chem.* 51(4), 590–600 (2021).
<https://doi.org/10.1080/24701556.2020.1799405>
- Goktas, A., Tumbul, A., Aslan, F., A new approach to growth of chemically depositable different ZnS nanostructures, *J. Sol-Gel Sci. Technol.* 90(3), 487–497 (2019).
<https://doi.org/10.1007/s10971-019-04990-9>
- Hussein M. Hussein, Structural and Optomagnetic Properties of Ni-Doped ZnS Synthesized by Solvothermal Method, *Colloid J.* 85(4), 666–672 (2023).
<https://doi.org/doi:10.1134/S1061933X22600610>
- Jadraque, M., Evtushenko, A. B., Ávila-Brandé, D., López-Arias, M., Loriot, V., Shukhov, Y. G., Kibis, L. S., Bulgakov, A. V., Martín, M., Co-Doped ZnS Clusters and Nanostructures Produced by Pulsed Laser Ablation, *J. Phys. Chem. C* 117(10), 5416–5423 (2013).
<https://doi.org/10.1021/jp3108792>
- Jindal, S., Sharma, P., Magnetic and optical properties of transition metal (Fe, Co) and rare-earth (Tb, Dy) doped ZnS nanoparticles, *J. Alloys Compd.* 879, 160383 (2021).
<https://doi.org/10.1016/j.jallcom.2021.160383>
- Kalantari, S., Shokuhfar, A., On the diverse utility of Cu doped ZnS/Fe₃O₄ nanocomposites, *Sci. Rep.* 14(1), 11669 (2024).
<https://doi.org/doi:10.1038/s41598-024-62611-0>
- Khan, M. M., Abdulwahab, K. O., Metals- and non-metals-doped ZnS for various photocatalytic applications, *Mater. Sci. Semicond. Process.* 181, 108634 (2024).
<https://doi.org/doi:10.1016/j.mssp.2024.108634>
- Khorsand Zak, A., Majid, W. H. A., Ebrahimizadeh Abrishami, M., Yousefi, R., Parvizi, R., Synthesis, magnetic properties and X-ray analysis of Zn_{0.97}X_{0.03}O nanoparticles (X = Mn, Ni, and Co) using Scherrer and size–strain plot methods, *Solid State Sci.* 14(4), 488–494 (2012).
<https://doi.org/10.1016/j.solidstatesciences.2012.01.019>
- Mani, S. K., Saroja, M., Venkatachalam, M., Rajamanickam, T., Antimicrobial Activity and Photocatalytic Degradation Properties of Zinc Sulfide Nanoparticles Synthesized by Using Plant Extracts, *J. Nanostructures* 8(2), 107–118 (2018).
<https://doi.org/10.22052/JNS.2018.02.001>
- Othman, A. A., Osman, M. A., Ali, M. A., Mohamed, W. S., Ibrahim, E. M. M., Sonochemically synthesized Ni-doped ZnS nanoparticles: structural, optical, and photocatalytic properties, *J. Mater. Sci. Mater. Electron.* 31(2), 1752–1767 (2020).
<https://doi.org/10.1007/s10854-019-02693-z>
- Palve, A. M., Deposition of Zinc Sulfide Thin Films From Zinc(II) Thiosemicarbazones as Single Molecular Precursors Using Aerosol Assisted

- Chemical Vapor Deposition Technique, *Front Mater.*, 6 (2019).
<https://doi.org/10.3389/fmats.2019.00046>
- Ramasamy, V., Praba, K., Murugadoss, G., Synthesis and study of optical properties of transition metals doped ZnS nanoparticles, *Spectrochim. Acta Part A Mol. Biomol. Spectrosc.* 96, 963–971 (2012).
<https://doi.org/10.1016/j.saa.2012.07.125>
- Rana, M. S., Das, S. K., Rahman, M. O., Ahmed, F., Hossain, M. A., Vanadium Doped ZnS Nanoparticles: Effect of Vanadium Concentration on Structural, Optical and Electrical Properties, *Trans. Electr. Electron. Mater.* 22(5), 612–621 (2021).
<https://doi.org/10.1007/s42341-020-00265-1>
- Reza Gholipour, M., Dinh, C.-T., Béland, F., Do, T.-O., Nanocomposite heterojunctions as sunlight-driven photocatalysts for hydrogen production from water splitting, *Nanoscale* 7(18), 8187–8208 (2015).
<https://doi.org/10.1039/C4NR07224C>
- Riazian, M., Yousefpoor, M., Photocatalytic activity, nanostructure and optical properties of 3D ZnS urchin-like via hydrothermal method, *Int. J. Smart Nano Mater.* 11(1), 47–64 (2020).
<https://doi.org/doi:10.1080/19475411.2019.1710001>
- Rose, M. M., Christy, R. S., Benitta, T. A., Kumaran, J. T. T., Bindhu, M. R., Phase transition in ZnS nanoparticles: electrical, thermal, structural, optical, morphological, antibacterial and photocatalytic properties, *Chalcogenide Lett.* 19(11), 855–869 (2022).
<https://doi.org/10.15251/CL.2022.1911.855>
- Sabaghi, V., Davar, F., Fereshteh, Z., ZnS nanoparticles prepared via simple reflux and hydrothermal method: Optical and photocatalytic properties, *Ceram. Int.* 44(7), 7545–7556 (2018).
<https://doi.org/10.1016/j.ceramint.2018.01.159>
- Shahid, R., Toprak, M. S., Muhammed, M., Microwave-assisted low temperature synthesis of wurtzite ZnS quantum dots, *J. Solid State Chem.* 187, 130–133 (2012).
<https://doi.org/10.1016/j.jssc.2012.01.007>
- Shanmugam, N., Cholan, S., Kannadasan, N., Sathishkumar, K., Viruthagiri, G., Effect of polyvinylpyrrolidone as capping agent on Ce³⁺ doped flowerlike ZnS nanostructure, *Solid State Sci.* 28, 55–60 (2014).
<https://doi.org/10.1016/j.solidstatesciences.2013.12.008>
- Shobana, T., Venkatesan, T., Kathirvel, D., A Comprehensive Review on Zinc Sulphide Thin Film by Chemical Bath Deposition Techniques, *J. Environ. Nanotechnol.* 9(1), 50–59 (2020).
<https://doi.org/10.13074/jent.2021.03.201394>
- Song, S., Xing, Z., Zhao, H., Li, Z., Wei Zhou, Recent advances in bismuth-based photocatalysts: Environment and energy applications, *Green Energy Environ.* 8(5), 1232–1264 (2023).
<https://doi.org/10.1016/j.gee.2022.04.004>
- Sousa, D. M., Alves, L. C., Marques, A., Gaspar, G., Lima, J. C., Ferreira, I., Facile Microwave-assisted Synthesis Manganese Doped Zinc Sulfide Nanoparticles, *Sci. Rep.* 8(1), 15992 (2018).
<https://doi.org/10.1038/s41598-018-34268-z>
- Shobana, T., Saravanan, R. S. S., Kathirvel, D., Effect of Copper Inclusion in Zinc sulfide Thin Films for Photocatalytic Applications, *J. Environ. Nanotechnol.* 13(1), 234–242 (2024).
<https://doi.org/10.13074/jent.2024.03.241539>
- Tounsi, A., Talantikite-Touati, D., Khalfi, R., Merzouk, H., Haddad, H., Optical and Structural Properties of ZnS:La Thin Films Elaborated by Sol-Gel Method, In: Proceedings of the Third International Symposium on Materials and Sustainable Development. Springer International Publishing, Cham, pp 44–51, (2018).
https://doi.org/10.1007/978-3-319-89707-3_6
- Wang, W., Lee, G.-J., Wang, P., Qiao, Z., Liu, N., Wu, J. J., Microwave synthesis of metal-doped ZnS photocatalysts and applications on degrading 4-chlorophenol using heterogeneous photocatalytic ozonation process, *Sep. Purif. Technol.* 237, 116469 (2020).
<https://doi.org/10.1016/j.seppur.2019.116469>
- Yang, M.-Q., Han, C., Xu, Y.-J., Insight into the Effect of Highly Dispersed MoS₂ versus Layer-Structured MoS₂ on the Photocorrosion and Photoactivity of CdS in Graphene–CdS–MoS₂ Composites, *J. Phys. Chem. C* 119(49), 27234–27246 (2015).
<https://doi.org/10.1021/acs.jpcc.5b08016>
- Yu, L., Ruan, H., Zheng, Y., Li, D., A facile solvothermal method to produce ZnS quantum dots-decorated graphene nanosheets with superior photoactivity, *Nanotechnology* 24(37), 375601 (2013).
<https://doi.org/10.1088/0957-4484/24/37/375601>
- Zhang, J., Liu, S., Yu, J., Jaroniec, M., A simple cation exchange approach to Bi-doped ZnS hollow spheres with enhanced UV and visible-light photocatalytic H₂-production activity, *J. Mater. Chem.* 21(38), 14655 (2011).
<https://doi.org/10.1039/c1jm12596f>